15th International Symposium on Flow Visualization
June 25-28, 2012, Minsk, Belarus

EFFECT OF LIQUID-BRIDGE SHAPE ON THE INSTABILITY OF MARANGONI CONVECTION IN SPACE EXPERIMENT

T. YANO[1], K. NISHINO[1,c], H. KAWAMURA[2], I. UENO[3], S. MATSUMOTO[4]

[1]Department of Mechanical Engineering, Yokohama National University, Yokohama 240-8501, Japan
[2]Department of Mechanics and System Design, Tokyo University of Science, Suwa 391-8502, Japan
[3]Department of Mechanical Engineering, Tokyo University of Science, Noda 278-8501, Japan
[4]Japan Aerospace Exploration Agency, Tsukuba 305-8505, Japan

[c]Corresponding author: Tel.&FAX: +81-45-339-3900; Email: nish@ynu.ac.jp

KEYWORDS:
Main subjects: flow visualization, space experiment, flow instability, Marangoni convection
Fluid: silicone oil, liquid bridge
Visualization method(s): tracer method
Other keywords: oscillation, aspect ratio, volume ratio

ABSTRACT: The effect of liquid-bridge shape on the instability of Marangoni convection has been studied through flow visualization conducted in space experiment. Liquid bridges of silicone oil with various volume ratios are generated in microgravity. They are suspended between coaxial disks 30mm or 50mm in diameter. No liquid-bridge deformation due to gravity is present in microgravity. The volume ratio, *VR*, denotes the ratio of the liquid volume to the volume of the gap between the disks. Marangoni convection is generated by the temperature difference imposed to the disks. The onset of oscillation from a steady laminar flow to an oscillatory 3-D flow is determined through flow visualization based on the tracer method. The effect of *VR* on the critical Marangoni number for the onset of oscillation is plotted. These are the first experimental data taken from non-deformed liquid bridges for various *VR*s. The present data differ from the data taken in terrestrial condition (i.e., 1g), indicating a significant effect of the gravity on the instability.

INTRODUCTION

Marangoni convection is driven by the surface-tension gradient along a liquid-gas interface. The surface tension, σ, is dependent on temperature, concentration and electric potential of the liquid-gas interface. As σ usually depends negatively on the temperature of the fluid, the driving force due to surface-tension gradient is directed from the cooler side toward the warmer side of the liquid-gas interface. Marangoni convection becomes of particular importance in small-scale flow systems such as liquid films, droplets, bubbles and liquid bridges.

The liquid bridge (LB, hereafter) is the geometry that is originally seen in the floating-zone method for crystal growth, as illustrated in Fig. 1a. This method is for manufacturing high-quality single crystals of high purity. The feed material is heated by a ring heater and the melt is suspended between the feed rod and the grown crystal. The temperature difference between the melting region and the solidified region is the driving force for the Marangoni convection. This flow configuration is modeled to a LB suspended between two coaxial disks with different temperatures, as illustrated in Fig. 1b. This simplified geometry is called the half-zone model. The temperature difference between the disks, ΔT, drives a flow that is directed from the heated disk toward the cooled disk along the surface and returns inside the LB. This geometry is now recognized as one of the basic flow fields for the study of thermocapillary convection and its instability mechanisms. It should be mentioned here that the fluids considered in the floating-zone method are of low *Pr* such as Si melt and GaSb melt while those considered in the half-zone model are of high *Pr* such as silicone oil and n-decane. The high *Pr* fluids are chosen for their being suitable for laboratory experimentation and visualization.

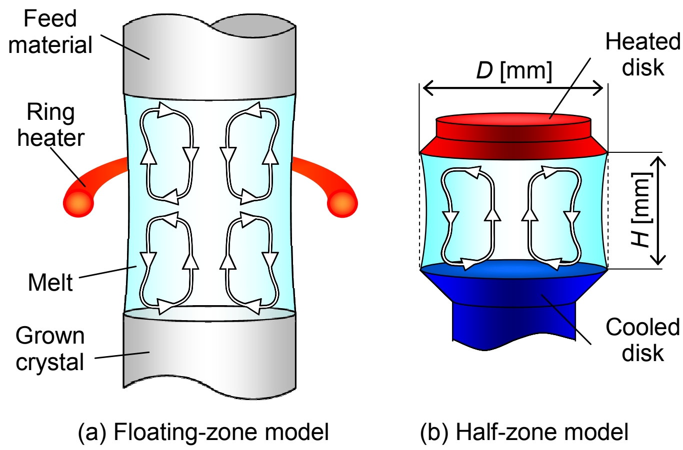

Fig. 1 Marangoni convection (a) in the floating-zone model and (b) in the half-zone model.

It is well known that the Marangoni convection in a LB changes from a steady, axisymmetric state to an oscillatory, non-axisymmetric one if ΔT exceeds a certain critical value. The appearance of such an unsteady flow causes the deterioration of the quality in the grown crystal. The onset of this instability is a function of many parameters as listed below:

fluid properties such as *Pr* number,
aspect ratio of the LB, *AR*,
volume ratio of the LB, *VR*, and
ambient gas conditions.

Here, *AR* is defined as $AR=H/D$ where H is the length of LB and D is the disk diameter, and *VR* is defined as V/V_0 where V is the volume of LB and V_0 is the volume of the cylindrical gap between the disks. The present paper focuses on the effect of *VR* on the instability of the Marangoni convection in LBs formed in microgravity.

To date, the effect of *VR* has been studied experimentally by Hu et al [1] and Masud et al [2] in their 1g experiments and numerically by Chen and Hu [3]. Common features reported in those previous studies are (1) the convection becomes most stabilized at a certain *VR* at around 0.8-0.9, and (2) the azimuthal mode numbers of oscillatory flows observed in over critical conditions are different between VR<0.8-0.9 and VR>0.8-0.9. These features are ascribed to the fact that different instability components are stimulated primarily for different *VR*s. However, the reasons for such different (or selective) stimulation are not clarified in the previous 1g experiments where several other influential factors such as LB deformation, natural convection inside LB and natural convection in the ambient gas are avoidably present. For this reason, microgravity experiments can provide idealistic conditions for the study of the effect of *VR* on the instability mechanisms.

A series of microgravity experiments, called Marangoni Experiment in Space (MEIS), have been conducted as the first science experiment on the Japanese Experimental Module "KIBO" of the International Space Station (ISS). Four series of experiments, MEIS-1, 2, 4 and 3 were carried out in 2008, 2009, 2010 and 2011, respectively. The overview of MEIS-1, 2 and 4 was reported by Kawamura et al. [4] and Yano et al. [5]. The effect of *VR* was studied mainly in MEIS-3 and some preliminary results were obtained in MEIS-2 and -4. MEIS-3 was conducted in the period from September 20, 2011 to February 8, 2012. Its purpose is to accumulate the data on the following phenomena in large LBs (30mm in diameter and up to 60mm in length) that can be formed only in a long-period microgravity environment on ISS:

(1) to determine the critical temperature difference for the onset of oscillatory flow,
(2) to realize high Marangoni number conditions for high *Pr* fluid,
(3) to clarify the effects of *VR*, heating rate, hysteresis and cooled disk temperature, and
(4) to observe if the hydrothermal wave with azimuthal mode number m=0 appears.

The present paper aims at describing the effect of *VR* while reporting some other necessary results.

METHOD

Fluid Physics Experiment Facility.

All the experimental runs in MEIS have been performed in Fluid Physics Experiment Facility (FPEF). The test fluid is silicone oil manufactured by Shin-Etsu Chemical Co., Ltd. The fluid is supplied from an exchangeable liquid cassette by using a precise injection mechanism. The mechanism also has suction capability for accurate adjustment of the liquid volume.

FPEF is designed to form a liquid bridge between two concentric disks; one is made of sapphire and the other is made of aluminum, both having the same diameter. It is 30mm in MEIS-1 and 2 while it is 50mm in MEIS-3 and 4. The sapphire disk is transparent and can be heated up to 90°C. The back-side surface of the sapphire disk, which is not the surface that is in contact with the liquid, is coated with a transparent ITO film for electric resistance heating. The temperature uniformity of the front surface of the sapphire disk is verified to be within ±0.5°C. The surface temperature is measured with two flush-mounted ITO film sensors which are calibrated on the ground before launch and corrected for any residual bias before each series of experiments. The aluminum disk is cooled with a Peltier element and its temperature is measured with three imbedded thermocouple sensors. The uniformity of the surface of the cooled disk is within ±0.1°C. Consequently, the temperature difference, ΔT, between the disks is defined with sufficient accuracy. The maximum length of the liquid bridge formed in FPEF is either 60mm for 30mm disk diameter or 62.5mm for 50mm disk diameter, giving the maximu *AR* of either 2.0 or 1.25, where *AR* is the ratio of the length, L, of the liquid bridge to the diameter of the disk, D.

Another important non-dimensional parameter representing geometry of liquid bridges is the volume ratio, *VR*, which defines the ratio of the volume of LB, V, to the cylindrical volume between the gap of the two disks, $V_0=\pi D^2 L/4$. In MEIS experiments, *VR*=0.95 is chosen as a typical value by considering that a value slightly lower than unity can stabilize long LBs against the g-jitters present in ISS. In MEIS-3 and 4, however, *VR* was varied in a wide range in order to examine the effect of *VR* on the instability mechanisms of Marangoni convection. The precise injection/suction mechanism mentioned above was used to make precise adjustment of *VR*.

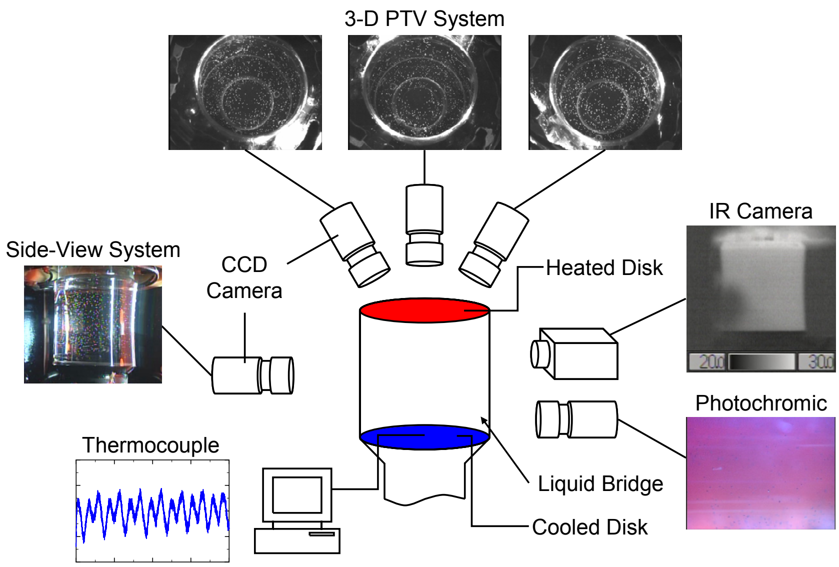

Fig. 2 Schematic image of experimental apparatuses installed in Fluid Physics Experiment Facility (FPEF)

The measurement apparatuses available in FPEF are schematically shown in Fig. 2. Three B/W CCD cameras are mounted near the heated disk so that they can provide multi-camera view of the flow in the liquid bridge through the transparent sapphire disk. This configuration is to make 3-D measurement of velocity field by using 3-D particle tracking velocimetry [6]. This technique is also used in the 1g experiments with small liquid bridges [7]. The shape of the liquid bridge and the overall flow pattern are viewed from the side of the liquid bridge by using a color CCD camera. Another color CCD camera is installed for photochromic dye activation technique [8] for the measurement of surface velocity of liquid bridge. This technique is used in MEIS-2 and 3 and the test fluid has a small quantity of photochromic dye (1',3',3'-trimethylindoline-2-Spiro-2- benzopyran: TNSB) dissolved in it at a concentration of 0.01-0.05wt%. Temperature measurements are made with an infrared camera and with a fine thermocouple sensor. The former is to measure the surface temperature of the liquid bridge, while the other which is placed on the cooled disk surface and immersed in the liquid is to measure the local fluid temperature.

Experimental conditions

The test fluids used in MEIS-1 and 2 are 5cSt silicone oil and those used in MEIS-3 and 4 are 20cSt silicone oil. Their physical properties are summarized in Table 1. As the test fluids for MEIS-2 and 3 contain a small quantity of TNSB (0.01-0.05wt%), its temperature coefficient of surface tension decreases slightly, as shown in Table 1. The temperature dependency of the kinematic viscosity of the test fluid is evaluated from the following equation [9]:

$$\frac{\nu}{\nu_{25}} = \exp\left(5.892\frac{25-T}{273.15+T}\right) \tag{1}$$

where ν_{25} and T are the kinematic viscosity at 25°C and the temperature considered, respectively. The Marangoni number from MEIS can be defined as below:

$$Ma = \frac{|\sigma_T|\Delta TH}{\rho\bar{\nu}\alpha} \tag{2}$$

where $\bar{\nu} = \{\nu(T_h)+\nu(T_c)\}/2$

The fluid is seeded with tracer particles for PTV measurements. These particles are metal-coated polymer particles that show good visibility and dispersion capability in silicone oil. In MEIS-3, the mean diameter of the trace particles is 180μm and about 2,000 particles are introduced in the liquid bridge. This relatively large number of tracer particles is to facilitate the observation of particle accumulation structure (PAS) that is expected to be formed in the liquid bridge. The liquid bridge is formed in a sealed chamber which is filled with argon gas at 94kPa and kept at about 21°C.

Table 1 Basic physical properties of the working fluids

Working fluid	5cSt silicon oil at 25°C	20cSt silicon oil at 25°C
Prandtl number, Pr (-)	67	207
density, ρ (kg·m^{-3})	915	950
kinematic viscosity, ν (m^2·s^{-1})	5.0×10^{-6}	20.0×10^{-6}
thermal diffusivity, α (m^2·s^{-1})	7.46×10^{-8}	9.67×10^{-8}
surface tension, σ (N·m^{-1})	19.7×10^{-3}	20.6×10^{-3}
temp. conf. of σ, σ_T (N·m^{-1} K^{-1})	-6.58×10^{-5} [a] -6.23×10^{-5} [b]	-6.24×10^{-5} [c] -5.85×10^{-5} [d]

[a] MEIS-1, [b] MEIS-2, [c] MEIS-4, [d] MEIS-3

RESULTS AND DISCUSSION

Instability of thermocapillary convection

Figure 3 shows the measured critical temperature difference, ΔT_c, plotted as a function of AR. All the results obtained from MEIS-1 through MEIS-4 are included. ΔT_c decreases with AR for AR<0.6 then starts to increase for AR>0.6 and takes a local peak at around AR=0.87. For AR>0.87, ΔT_c decreases and seems to asymptote to a nearly constant value, which depends on the experimental conditions. The results of MEIS-1 and 2, both using 5cSt silicone oil and 30mm disk diameter, are in good agreement with each other while the results of MEIS-3 and 4, both using 20cSt silicone oil, show appreciably larger values than those of MEIS-1 and 2. This difference should be due to the difference in *Pr* as well as in the size of the LB (30mm vs. 50mm in disk diameter).

For better understanding, ΔT_c is non-dimensionalized into the critical Marangoni number, Ma_c, and plotted as a function of *AR* as shown in Fig. 4. Qualitatively speaking, all the data for *AR*<1.12 show a similar distribution in the sense that they have a local minimum at *AR*=0.63 and a local maximum at *AR*=0.87 even though the value of the local maximum seems to depend on the experimental conditions. There is, however, a notable difference between the results of MEIS-2 and MEIS-4 in the value of Ma_c at *AR*=1.25; the former shows a second local maximum while the latter does not show such a maximum. As they used the same disk diameter (30mm), this difference should be ascribed to the difference in the working fluids (5cSt silicone oil in MEIS-2 while 20cSt silicone oil in MEIS-4). For *AR*>1.5, Ma_c from both MEIS-2 and 4 shows a consistently increasing behavior.

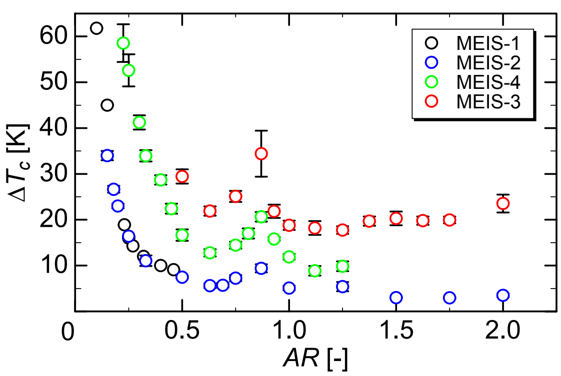

Fig. 3 ΔT_c vs. *AR*

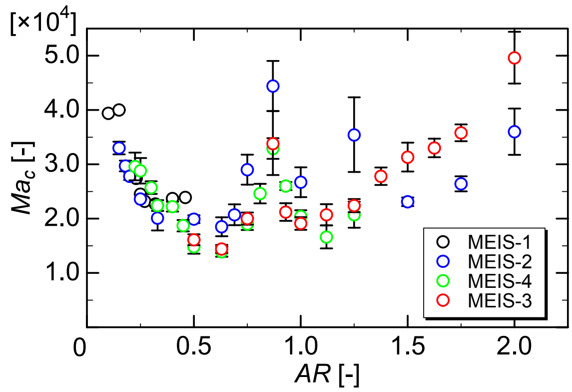

Fig. 4 *Ma* vs. *AR*

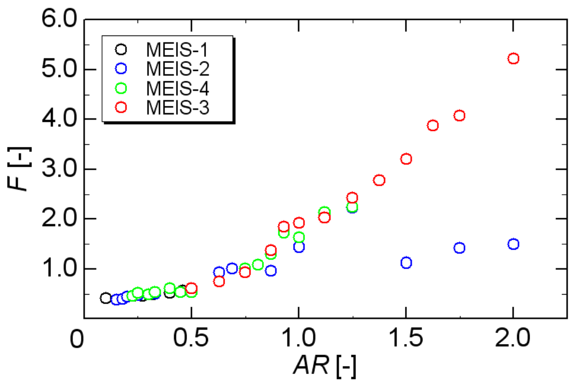

Fig. 5 *F* vs. *AR*

Figure 5 shows the non-dimensional oscillation frequency, *F*, plotted as a function of *AR*, where *F* is defined as follows [10]:

$$F = \frac{H^2}{\alpha\sqrt{Ma}} f \tag{3}$$

where *f* is the measured dimensional oscillation frequency. For *AR*<1.25, all the results from MEIS-1 through MEIS-4 collapse to a single curve that shows a monotonic increase with *AR*. For *AR*>1.25, however, *F* from MEIS-3 continues to follow the same curve while *F* from MEIS-4 shows a sudden decrease. The reason for this sudden decrease is the appearance of the longitudinal oscillation mode in which multiple vortical structures start to exist in the axial direction in long LBs [11]. The continuous increase of *F* observed in MEIS-3 suggests that such a transition to the longitudinal mode does not occur in long LBs of 20cSt silicone oil. This should be clarified in the detailed analysis of the data taken in MEIS-3.

Effect of volume ratio

The effect of volume ratio, *VR*, on the instability mechanism is one of the main research targets of MEIS-3. To study this effect, *VR* was varied in the range from 0.45 to 1.08 for constant *AR* (=0.5) as shown in Fig. 6. This wide range of *VR* is chosen because it was found in MEIS-4 where *VR*=0.908-1.05 was examined that Ma_c was unexpectedly insensitive to *VR* in contrast to what was reported in the previous 1g experiments [1, 2, 3] where Ma_c was found to be sensitive to a small change of *VR* near 0.90.

In MEIS, the liquid volume, *V*, is precisely controlled by using the liquid injection/suction mechanism mentioned above. In Fig. 7, the image of LB for *AR*=1.0 and *VR*=0.70 acquired in MEIS-3 is compared with the shape that is calculated from the Young-Laplace equation with neglecting the effect of gravity. There is good agreement between the LB image and the calculated shape, thus indicating that a LB having an idealistic shape without deformation is generated in microgravity.

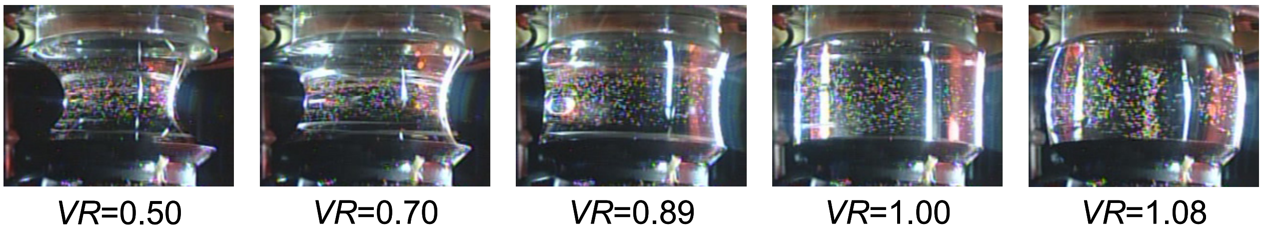

Fig. 6 Shapes of liquid bridge for different *VR* and constant *AR* (=0.5).

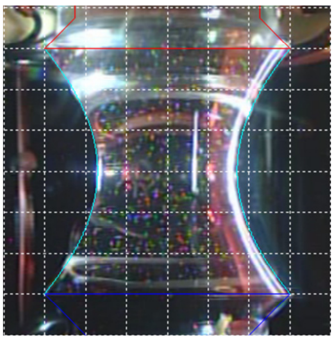

Fig. 7 Comparison of the LB image for *AR*=1.0 and *VR*=0.70 to the calculated shape.

The measured Ma_c is plotted as a function of *VR* for *AR*=0.35, 0.5 and 1.0 in Fig. 8. Also shown here are the data taken on the ground for *AR*=0.5 and *D*=5mm with 5cSt and 20cSt silicone oils. As mentioned above, these data taken in 1g show a clear peak at around *VR*=0.85, indicating the Marangoni convection is most stabilized at this *VR*. In contrast, the data taken in MEIS-3 for *AR*=0.5 with 20cSt silicone oil show a peak at *VR*=0.53, which is substantially smaller than *VR*=0.85. Preliminary data taken in MEIS-4 (*AR*=0.5, *D*=50mm and 20cSt silicone oil) and in MEIS-2 (*AR*=0.5, D=30mm and 5cSt silicone oil) follow the trend seen in the data taken from MEIS-3. The peak position for *AR*=1.0 in MEIS-3 is located at *VR*=0.7 while no peak for *AR*=0.35 is observed. The non-dimensional oscillation frequency, *F*, is plotted as a function of VR in Fig. 9. It is seen that *F* increases monotonously in the range of *VR* examined and that the representative value of *F* is roughly the same as the value of *AR*.

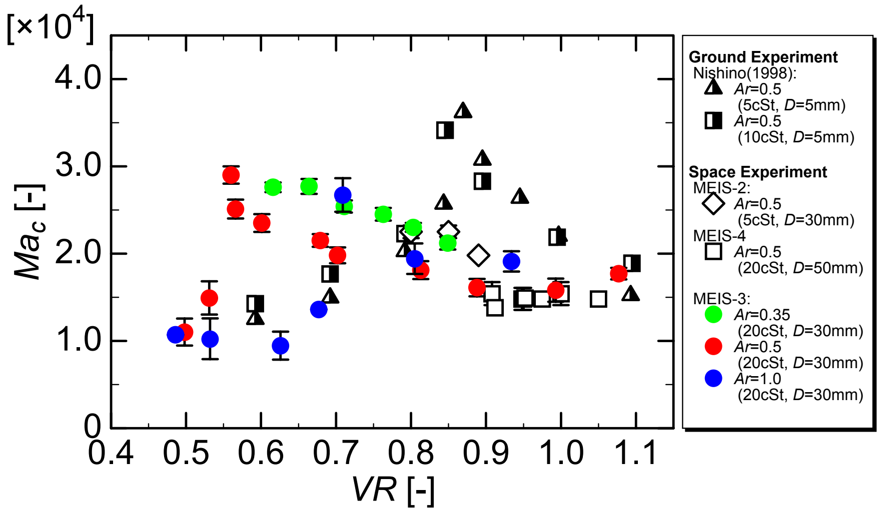

Fig. 8 Critical Marangoni number plotted as a function of *VR*.

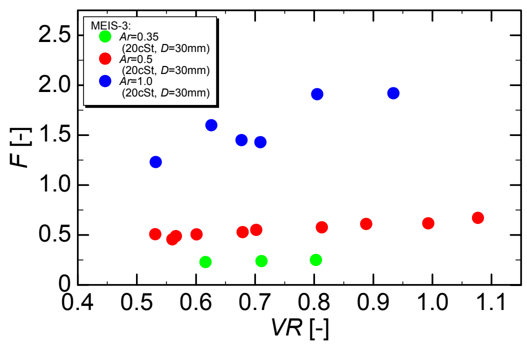

Fig. 9 Non-dimensional oscillation frequency plotted as a function of *VR*.

Here, it is interesting to examine the effect of gravity on the shape of LB. Figure 10 shows comparison of LB shapes between μg and 1g, both shapes being calculated from the Young-Laplace equation. The LB considered here has *AR*=0.5 and *D*=5mm. This is a typical size of LB formed in 1g experiment. It is seen that the deformation of LB shape due to gravity is not so remarkable for all *VR*s shown here. This may suggest that the difference in the effect of *VR* on Ma_c between μg and 1g is not the direct consequence of the change of LB shape but the result of other factor(s) affected by the gravity such as the natural convection inside the liquid bridge, the natural convection in the surrounding gas, and so on.

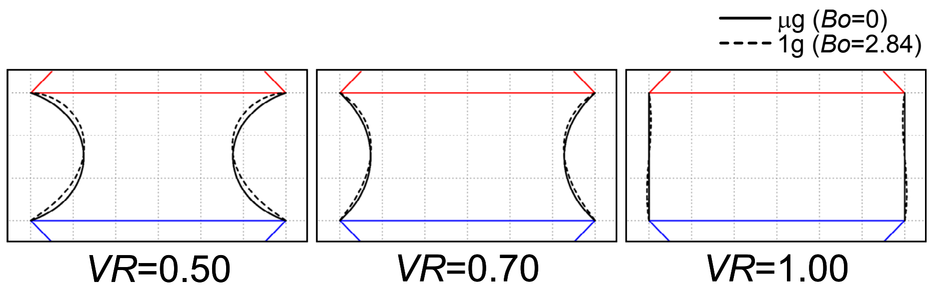

Fig. 8 Comparison of LB shape between μg and 1g for *AR*=0.5 and *D*=5mm.

The mode of osciilation is examined from the visualization images data taken in MEIS-3. It was determined from the end-view images of tracer particles taken through the transparent heated disk as shown in Fig. 9. These images are taken for *AR*=0.5 and *VR*=0.50, 0.70 and 1.00. As depicted in the figure, a rotating mode of oscillation is observed for *VR*=0.50 while standing modes of oscillation are observed for *VR*=0.70 and 1.00. Note that the peak of Ma_c for this aspect ratio exists at *VR*=0.53. The relation between Ma_c and the mode of oscillation is plotted as a function of *VR* for *AR*=0.50 and 1.0 in Figs. 10 and 11, respectively. It is clearly recognized that *VR* for the peak of Ma_c corresponds to the change of oscillation modes from rotating mode to standing mode.

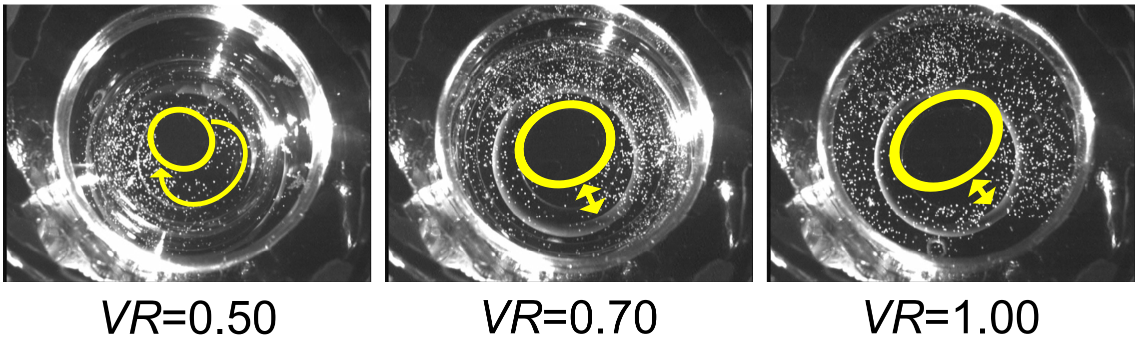

Fig. 9 End-view visualization images of tracer particles taken through the transparent heated disk.

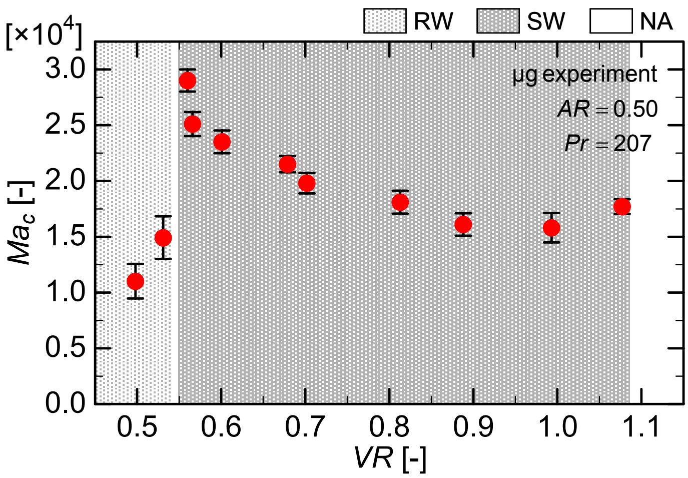

Fig. 10 Relation between Ma_c and mode of oscillation for *AR*=0.50 and 20cSt silicone oil.

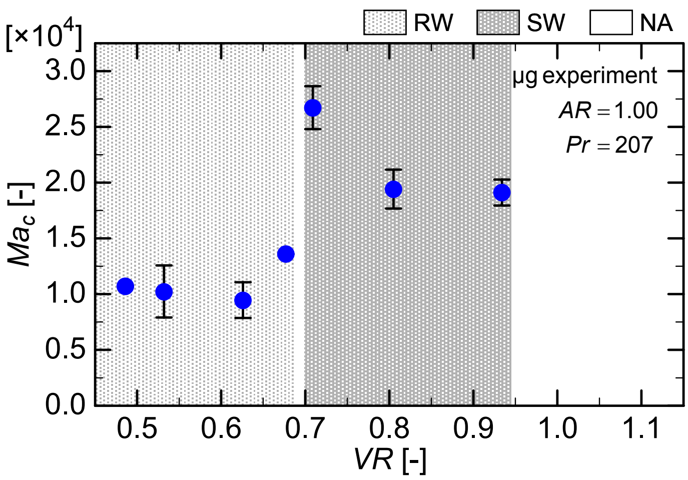

Fig. 11 Relation between Ma_c and mode of oscillation for *AR*=1.0 and 20cSt silicone oil.

EFFECT OF LIQUID-BRIDGE SHAPE ON THE INSTABILITY OF MARANGONI CONVECTION IN SPACE EXPERIMENT

CONCLUSIONS

This paper reports the effect of liquid-bridge shape on the instability of Marangoni convection generated in microgravity on the international space station (ISS). Long liquid bridges of silicone oil (5cSt and 20cSt) are generated in microgravity. They are suspended between coaxial disks 30mm or 50mm in diameter. No liquid-bridge deformation due to gravity is present in microgravity. The effect of the liquid-bridge shape is studied by change the volume ratio, *VR*, which denotes the ratio of the liquid volume to the volume of the gap between the disks. Marangoni convection is generated by the temperature difference imposed to the disks. The onset of oscillation from a steady laminar flow to an oscillatory 3-D flow is determined through flow visualization based on the tracer method. The effect of *VR* on the critical Marangoni number for the onset of oscillation is plotted. These are the first experimental data taken from non-deformed liquid bridges for various *VR*s.

The present data taken in microgravity (μg) differ from the data taken on ground (i.e., 1g), indicating a significant effect of the gravity on the instability. It is shown that the convection in μg is most stabilized at a certain *VR* whose value is, however, much smaller than that observed in the previous 1g experiments. It is conjectured that this difference between μg and 1g is not due to the direct consequence of the gravity-induced deformation of liquid bridges but due to the difference in other factors such as the natural convection inside and outside the liquid bridge. It is found that the mode of oscillation changes from a rotating mode to a standing mode at the *VR* that gives the largest critical Marangoni number.

ACKNOWLEDGEMENT

The author would like to thank JAXA and the members of MEIS for their assistance to perform this study. The author also acknowledges that a part of this study was supported by KAKENHI (Grant-in-Aid for Scientific Research (B), 24360078) from the Japan Society for the Promotion of Science (JSPS).

REFERENCES

1. Hu WR, Shu JZ, Zhou R, Tang ZM, Influence of liquid bridge volume on the onset of oscillation in floating zone convection I. Experiments, Journal of Crystal Growth, Vol. 142, Issues 3–4, pp. 379–384, 1994.
2. Masud J, Kamotani Y, Ostrach S, Oscillatory thermocapillary flow in cylindrical columns of high Prandtl number fluids, Journal of Thermophysics and Heat Transfer, Vol. 11, No. 1, pp. 105-111, 1997.
3. Chen QS, Hu WR, Influence of liquid bridge volume on instability of floating half zone convection, International Journal of Heat and Mass Transfer, Vol. 41, Issues 6–7, pp. 825–837, 1998.
4. Kawamura H, Nishino K, Matsumoto S, Ueno I. Report on microgravity experiments of Marangoni convection aboard international space station, Transactions of ASME, Journal of Heat Transfer, Vol. 134, pp. 031005-031018, 2012.
5 Yano T, Nishino K, Kawamura H, Ueno I, Matsumoto S, Ohnishi M, Sakurai M, Space experiment on the instability of Marangoni convection in large liquid bridge - MEIS-4: Effect of Prandtl number - , Journal of Physics, Vol. 327, pp. 012029-012036, 2011.
6. Nishino K, Kasagi N, Hirata M, Three-dimensional particle tracking velocimetry based on automated digital image processing, Transactions of ASME, Journal of Fluids Engineering, Vol. 111, pp. 384-391, 1989.
7. Nishimura M, Ueno I, Nishino K, Kawamura H, 3D PTV measurement of oscillatory thermocapillary convection in half-zone liquid bridge, Experiments in Fluids, Vol. 38, No. 3, pp. 285-290, 2005.
8. Kawaji M, Ahmad W, DeJesus JM, Sutharshan B, Lorencez C, Ojha M, 1993, Flow visualization of two-phase flows using photochromic dye activation method, Nuclear Engineering and Design, Vol. 141, pp. 343-355, 1993.
9. Shin-Etsu, Chemical Co. Ltd., 2004, Silicone Fluid (product catalogue), pp. 12-13.
10. Preisser F, Schwabe D, Scharmann A, Steady and oscillatory thermocapillary convection in liquid columns with free cylindrical surface, Journal of Fluid Mechanics, Vol. 126, pp. 545-567, 1983.
11. Yano T, Nishino K, Kawamura H, Ueno I, Matsumoto S, Ohnishi M, Sakurai M, 3-D PTV measurement of Marangoni convection in liquid bridge in space experiment, Experiments in Fluids, DOI 10.1007/s00348-011-1136-9, 2011.